

## Measuring Amide Nitrogen Quadrupolar Coupling by High-Resolution $^{14}\text{N}/^{13}\text{C}$ NMR Correlation under Magic-Angle Spinning

Zhehong Gan

National High Magnetic Field Laboratory, 1800 East Paul Dirac Drive, Tallahassee, Florida 32310

Received November 30, 2005; E-mail: gan@magnet.fsu.edu

Along with hydrogen, carbon, and oxygen, the nitrogen atom constitutes one of the most important elements in organic, inorganic, and biological molecules. Among the two nitrogen isotopes,  $^{15}\text{N}$  NMR spectroscopy (0.37% natural abundance) has been used extensively with favorable NMR properties of a spin-1/2, while the more abundant  $^{14}\text{N}$  isotope (99.6%) has rarely been studied. The useful information on nitrogen electric field gradient (EFG) is accessible only through  $^{14}\text{N}$  quadrupolar coupling which usually dominates over other spin interactions.<sup>1–7</sup> Direct NMR detection of  $^{14}\text{N}$  suffers from poor sensitivity and broad lines due to low- $\gamma$  properties and large quadrupolar interaction. The integer  $^{14}\text{N}$  spin precludes the presence of a single-quantum central-transition as observed for half-integer quadrupolar nuclei without the broadening from the first-order quadrupolar interaction. Observation of the overtone ( $1 \leftrightarrow -1$ ) transition, both directly<sup>8–11</sup> and indirectly,<sup>12,13</sup> can avoid the first-order quadrupolar broadening, but the overtone signal intensity and excitation are second-order effects that dwindle at high magnetic fields. This communication shows that indirect  $^{14}\text{N}$  detection through nearby  $^{13}\text{C}$  under magic-angle spinning (MAS) can overcome the resolution and sensitivity limitations for acquiring  $^{14}\text{N}$  NMR spectra of solids.  $^{14}\text{N}$  peaks under MAS display large isotropic second-order quadrupolar shifts with relatively small anisotropic broadening, such that  $^{14}\text{N}$  quadrupolar coupling can be measured precisely from the  $^{14}\text{N}$  peak positions relative to their chemical shifts. The high-resolution  $^{14}\text{N}/^{13}\text{C}$  correlation experiment under MAS and the measurement of amide nitrogen quadrupolar coupling are demonstrated with a natural abundant tripeptide Ala·Gly·Gly (AGG).

Figure 1 shows the slightly modified HMQC-type pulse sequence used for two-dimensional (2D)  $^{14}\text{N}/^{13}\text{C}$  correlation under magic-angle spinning. Both  $J$  and dipolar couplings contribute to the heteronuclear correlation. The scalar coupling is invariant under MAS, and typical coupling constants in proteins and polypeptides are  $J_{\text{NCO}}^1 \sim 11$  Hz,  $J_{\text{NCA}}^1 \sim 5\text{--}8$  Hz, and  $J_{\text{NCA}}^2 \sim 3\text{--}6$  Hz (note the scaling by  $\gamma$  relative to  $^{15}\text{N}$ ).<sup>14</sup> The slow buildup of two-spin coherence  $C_x \rightarrow \sin(\pi J \tau) C_y S_z$  competes with the decay from  $^{13}\text{C}$   $T_2$  relaxation. The much larger dipolar coupling is modulated by the sample rotation. The secular dipolar coupling term is averaged to zero under MAS. For  $^{14}\text{N}/^{13}\text{C}$  spin pairs, the nonsecular dipolar coupling terms are non-negligible due to the large  $^{14}\text{N}$  quadrupolar interaction. The second-order quadrupolar–dipolar interaction  $D_{\text{QC}}(S^2 - 3S_z^2)/3$  contains  $l = 0, 2, 4$  isotropic and anisotropic terms. Under MAS, the  $l = 0$  isotropic coupling<sup>15</sup>

$$D_{\text{Q}}^{\text{iso}} = \frac{9}{10} \frac{C_q}{v_{\text{N}}} d [(3 \cos^2 \vartheta_d - 1)/2 - \eta \sin^2 \vartheta_d \cos 2\varphi_d/2] \quad (1)$$

often dominates over the scaled  $l = 4$  anisotropic term, causing 2-to-1 ( $m = \pm 1, 0$ ) splitting to carbons directly bonded to  $^{14}\text{N}$ . This residual dipolar coupling has been frequently observed in  $^{13}\text{C}$  MAS spectra in the past at low magnetic fields.<sup>15–22</sup> A residual

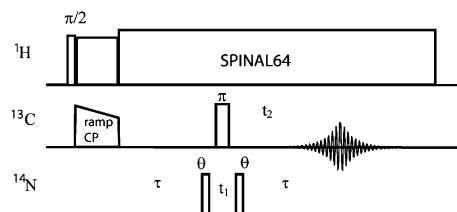


**Figure 1.** HMQC pulse sequence for  $^{14}\text{N}/^{13}\text{C}$  correlation under MAS. The evolution time  $t_1$  must be rotor-synchronized ( $t_1 + p\nu_{\text{N}14} = n\tau_r$ ) and the magic-angle needs to be set precisely for a complete average of the first-order quadrupolar shift. A phase cycle  $\varphi = +x, -x$  (real) +  $y, -y$  (imaginary) of the  $^{14}\text{N}$  pulses and a receiver phase  $+x, -x$  selects the single-quantum transition.

dipolar coupling of  $\sim 120$  Hz was measured for the amide nitrogen in *N*-acetyl-L-valine at 3.53T.<sup>19</sup> At 14.1T (600 MHz magnet), the residual dipolar coupling is expected to be  $\sim 30$  Hz, significantly larger than the  $J$  coupling constants.

Figure 2 shows the 2D  $^{14}\text{N}/^{13}\text{C}$  correlation spectrum of AGG. All expected peaks of direct-bonded  $^{14}\text{N}/^{13}\text{C}$  pairs are well separated by the  $^{13}\text{C}$  chemical shift. Along the indirect dimension, the  $^{14}\text{N}$  peaks show large shifts from their isotropic chemical shift positions. These shifts along with the broadening are the result of the second-order quadrupolar effect. The much larger first-order quadrupolar interaction is averaged to zero by rotor synchronized  $t_1$  and a precisely set magic-angle, similar to the satellite-transition magic-angle spinning (STMAS) experiment of half-integer quadrupolar spins.<sup>23,24</sup> As the second-order quadrupolar shift has been well studied for half-integer quadrupolar nuclei, the  $l = 0, 2, 4$  expansion coefficients for  $S = 1$  spin are expressed here by their ratios to that of the central transition of half-integer spins<sup>24</sup>

$$R_0 = -4/5, R_2 = 1/10, R_4 = -2/15 \quad (2)$$

It is important to note that the ratios for the anisotropic terms  $R_2$  and  $R_4$  are much smaller than the isotropic term  $R_0$ . This difference makes the isotropic second-order quadrupolar shift<sup>24</sup>

$$\delta_{\text{Q}}^{\text{iso}} = \frac{1}{20} \left( \frac{\chi_q}{v_0} \right)^2, \chi_q = \frac{eQ}{h} \sqrt{V_{xx}^2 + V_{yy}^2 + V_{zz}^2} = \sqrt{\frac{3 + \eta^2}{2}} C_q \quad (3)$$

much larger than the anisotropic broadening. For nitrogen, the downfield quadrupolar shift can be easily separated from the chemical shift obtained by a  $^{15}\text{N}$  NMR MAS experiment.

For amide nitrogen, the quadrupolar shift can be over 600 ppm at 14.1 T (43.35 MHz  $\nu_{\text{N}}$ ) with quadrupolar coupling constant in the range of 3–4 MHz. Such large shifts can cause alias along the indirect  $^{14}\text{N}$  dimension as the spectral window is restricted to the spinning frequency with rotor-synchronized evolution time  $t_1$ . Spectral de-aliasing may be necessary when measuring the quadrupolar shift. With the large shifts and small broadening, the

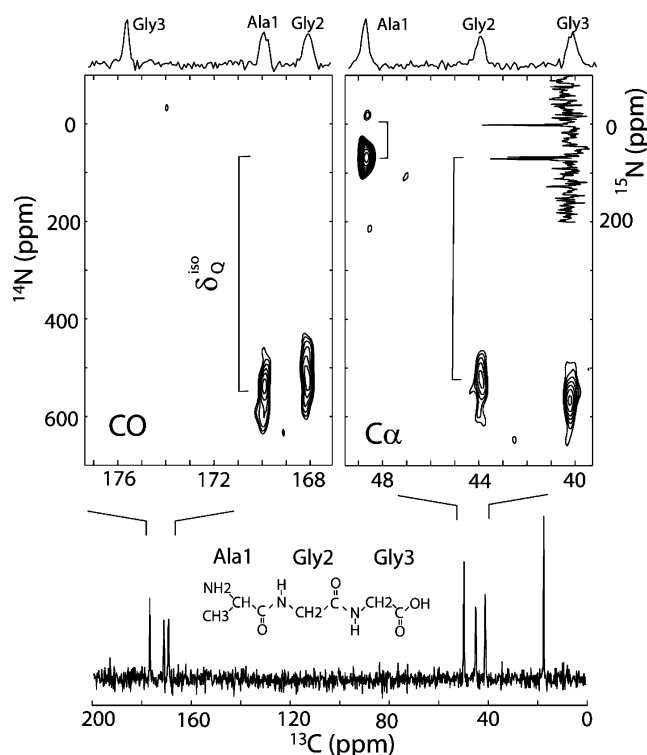


**Figure 2.**  $^{14}\text{N}/^{13}\text{C}$  correlation spectrum of natural abundant Ala·Gly·Gly (14.1T  $B_0$ , 600 MHz Bruker-DRX console, 15 ms  $\tau$ , 25 kHz MAS with 2.5 mm rotor, 16  $t_1$  increments, 8K scans, 2  $\mu\text{s}$   $^{14}\text{N}$  pulse with 50 kHz  $\nu_1$ , SPINAL64  $^1\text{H}$  decoupling with 125 kHz  $\nu_1$ ). The vertical brackets indicate the isotropic second-order quadrupolar shift  $\delta_Q^{\text{iso}}$  from the chemical shift measured by a separate  $^{15}\text{N}$  MAS experiment shown on the right. The nitrogen chemical shift is referenced to solid  $\text{NH}_4\text{Cl}$ . Because of the large second-order quadrupolar shifts, the amide  $^{14}\text{N}$  peaks have been de-aliased after doubling the spectral window from 25 to 50 kHz.

isotropic quadrupolar shift can be measured precisely for the determination of  $\chi_q = \sqrt{\text{trace}(Q \cdot Q^T)}$ , a parameter representing the magnitude of the quadrupolar coupling tensor  $Q$ . For AGG,  $\chi_q = 4.29 \pm 0.05$  and  $4.13 \pm 0.05$  MHz are obtained from the 490 and 454 ppm quadrupolar shifts, respectively, for Ala1 and Gly2 (the different quadrupolar shifts also assign the pairing of CO and C $\alpha$  connecting amide nitrogen in the polypeptide). The results are in good agreements with  $\chi_q = 4.32$  and 4.05 MHz calculated with  $C_q = 3.2 \pm 0.1$  and  $3.0 \pm 0.1$  MHz and  $\eta = 0.8 \pm 0.2$  reported in a previous study of AGG.<sup>25</sup> A determination of the asymmetry factor  $\eta$  from the second-order quadrupolar shift requires line shape fitting and was not attempted here because of limited  $t_1$  increments and signal-to-noise ratio.

Two factors are critical to the overall efficiency of the HMQC experiment that may offset the sensitivity gain of  $^{13}\text{C}$  detection. First, the two-spin coherence buildup requires a long mixing time  $\tau$  for the small  $J$  and residual dipolar couplings and is subject to  $^{13}\text{C}$   $T_2$  relaxation. High-power and multiple-pulse proton decoupling optimized for prolonging  $T_2^*$  helps to reduce this signal loss.<sup>26,27</sup> Second, by far the most loss occurs during the two  $^{14}\text{N}$  pulses because of the insufficient bandwidth with  $\nu_1 \approx 50$  kHz compared to the quadrupolar frequency offsets over 1 MHz (similar loss occurs in the case of direct  $^{14}\text{N}$  detection). Strong  $^{14}\text{N}$  pulses with small flip-angles ( $\theta \approx 35^\circ$ ) help to increase the bandwidth. The other reason for using small flip-angle pulses is for the two-spin coherence contribution from the residual dipolar coupling,  $\sin(\pi D_Q \tau) C_y (S^2 - 3S_z^2)/3$ . A  $90^\circ$  pulse transfers the coherence mostly to the  $^{14}\text{N}$  double-quantum transition, where a shorter pulse transfers more efficiently to the single-quantum transition. Another

modification to the HMQC pulse sequence is that the  $^{13}\text{C}$  acquisition starts immediately after the last  $^{14}\text{N}$  pulse. Full-echo acquisition with a long  $\tau$  increases the signal/noise ratio by  $\sim\sqrt{2}$ .<sup>28</sup>

In conclusion, the  $^{14}\text{N}/^{13}\text{C}$  correlation experiment via  $J$  and residual dipolar couplings under MAS overcomes the resolution and sensitivity limitations in acquiring  $^{14}\text{N}$  NMR spectra. The result of a model polypeptide demonstrates that large quadrupolar couplings up to 4 MHz, such as those of amide nitrogen, can be measured precisely from the isotropic second-order quadrupolar shift. In the past, little has been learned on nitrogen quadrupolar coupling for molecules with multiple nitrogen sites and large quadrupolar coupling constants. The indirect detection method has the advantages of high spectral resolution and sensitivity, making the measurement and the use of  $^{14}\text{N}$  quadrupolar coupling possible for large molecules. It should be mentioned that the measurement with AGG has been carried out with only  $\sim 1\%$  ( $^{13}\text{C}$  natural abundance) of the  $^{14}\text{N}$  spins in the sample. Isotope enrichment can increase the sensitivity by an order of magnitude for the use of  $^{14}\text{N}$  quadrupolar coupling in large and complex systems, such as proteins and nucleic acids.

**Acknowledgment.** This work has been supported by the National High Magnetic Field Laboratory through Cooperative Agreement (DMR-0084173) with the National Science Foundation and the State of Florida, and is dedicated to Professor David M. Grant, University of Utah, for his 75th birthday.

## References

- Jakobsen, H. J.; Bildsoe, H.; Skibsted, J.; Giavani, T. *J. Am. Chem. Soc.* **2001**, *123*, 5098–5099.
- Bastow, T. J.; Massiot, D.; Coutures, J. P. *Solid State Nucl. Magn. Reson.* **1998**, *10*, 241–245.
- Giavani, T.; Bildsoe, H.; Skibsted, J.; Jakobsen, H. J. *J. Magn. Reson.* **2004**, *166*, 262–272.
- Khitrin, A. K.; Fung, B. M. *J. Chem. Phys.* **1999**, *111*, 8963–8969.
- Hill, E.; Yesinowski, J. *J. Chem. Phys.* **1997**, *107*, 346–354.
- Siminovich, D. J.; Brown, M. F.; Jeffery, K. R. *Biochemistry* **1984**, *23*, 2412–2420.
- Santos, J.; Lee, D.; Ramamoorthy, A. *Magn. Reson. Chem.* **2004**, *42*, 105–114.
- Tycko, R.; Stewart, P. L.; Opella, S. J. *J. Am. Chem. Soc.* **1986**, *108*, 5419–5425.
- Tycko, R.; Opella, S. J. *J. Am. Chem. Soc.* **1986**, *108*, 3531–3532.
- Tycko, R.; Opella, S. J. *J. Chem. Phys.* **1987**, *86*, 1761–1774.
- Lee, D.; Ramamoorthy, A. *Chem. Phys. Lett.* **1997**, *280*, 501–506.
- Garroway, A. N.; Miller, J. B. *J. Magn. Reson.* **1989**, *82*, 591–596.
- Takegoshi, K.; Yano, T.; Takeda, K.; Terao, T. *J. Am. Chem. Soc.* **2001**, *123*, 10786–10787.
- Cavanagh, J.; Fairbrother, W.; Palmer, A.; Skelton, N. *Protein NMR Spectroscopy/Principles and Practice*; Academic Press: San Diego, CA, 1996; p 481.
- Gan, Z. H.; Grant, D. M. *J. Magn. Reson.* **1990**, *90*, 522–534.
- Vanderhart, D.; Gutowsky, H. S.; Farrar, T. C. *J. Am. Chem. Soc.* **1967**, *89*, 5056–5057.
- Hexem, J. G.; Frey, M. H.; Opella, S. J. *J. Am. Chem. Soc.* **1981**, *103*, 224–226.
- Naito, A.; Ganapathy, S.; McDowell, C. A. *J. Chem. Phys.* **1981**, *74*, 5393–5397.
- Hexem, J. G.; Frey, M. H.; Opella, S. J. *J. Chem. Phys.* **1982**, *77*, 3847–3856.
- Naito, A.; Ganapathy, S.; McDowell, C. A. *J. Magn. Reson.* **1982**, *48*, 367–381.
- Olivieri, A. C.; Frydman, L.; Diaz, L. E. *J. Magn. Reson.* **1987**, *75*, 50–62.
- Grey, C. P.; Eijkelenboom, A. P. A. M.; Veeman, W. S. *Solid State Nucl. Magn. Reson.* **1995**, *4*, 113–120.
- Gan, Z. H. *J. Am. Chem. Soc.* **2000**, *122*, 3242–3243.
- Gan, Z. H. *J. Chem. Phys.* **2001**, *114*, 10845–10853.
- Stewart, P. L.; Valentine, K. G.; Opella, S. J. *J. Magn. Reson.* **1987**, *71*, 45–61.
- Fung, B. M.; Khitritin, A. K.; Ermolaev, K. *J. Magn. Reson.* **2000**, *142*, 97–101.
- De Paepe, G.; Lesage, A.; Emsley, L. *J. Chem. Phys.* **2003**, *119*, 4833–4841.
- Iuga, D.; Morais, C.; Gan, Z. H.; Neuville, D. R.; Cormier, L.; Massiot, D. *J. Am. Chem. Soc.* **2005**, *127*, 11540–11541.

JA0578597